IRANIAN JOURNAL OF CATALYSIS

Steam reforming of propane over Ni-K/CeO_2-Al_2O_3 catalyst in fluidized- and fixed-bed reactors under low steam to propane ratio

Mir Mohammad Motiee[a], Golshan Mazloom[b,*], Seyed Mehdi Alavi[a]

[a]*Reaction Engineering Lab., Chemical Engineering Department, Iran University of Science and Technology, 16846-13114, Tehran, Iran*

[b]*Department of Chemical Engineering, Faculty of Engineering, University of Mazandaran, 13534-47416, Babolsar, Iran.*

Received 14 January 2020; received in revised form 6 September 2020; accepted 14 September 2020

ABSTRACT

Fluidized bed was employed to investigate propane steam reforming over Ni-K/CeO_2-Al_2O_3 catalyst. The catalyst was characterized by XRD, SEM, TG/DTA, and N_2 adsorption-desorption tests. Effects of promoters, space velocity, temperature, and steam/propane (S/C) ratio on propane conversion, H_2 yield, H_2/CO ratio, and stability were studied and discussed. The experiments were carried out under conditions which favored coke formation. The reaction in the fluidized bed was compared with the reaction in a conventional fixed bed reactor. Obtained results indicated that fluidization and continuous circulation of catalyst induced back-mixing phenomena, increasing contact rate between catalysts and feed, uniform distribution of temperature, and steam concentration. As a result, higher conversion, H_2 yield, and significant suppression of coke deposition were observed in the fluidized bed at all of the experimental conditions. The fluidized bed catalyst also exhibited good regenerability by restoring its initial catalytic activity after one h of regeneration in air. It was shown that fluidization could compensate for the lack of water and enhance coke gasification. At S/C=3, the catalytic performance in both reactors was almost stable. With decreasing S/C to 2.5, the activity in the fixed bed decreased rapidly. While the stability was more pronounced in the fluidized bed. At S/C=1.5, the catalyst at both reactors deactivated fast due to the lower H/C ratio, massive coke formation, and poor fluidization.

***Keywords**: Fluidized bed, Steam reforming, Propane, Coke formation.*

1. Introduction

By increasing global concerns about the environmental contaminations, hydrogen has attracted much attention as an effective and clean energy source [1]. In addition, hydrogen and syngas are the raw materials frequently used in the production of liquid fuels and oxygenated products [2, 3]. Nowadays, the most common routes for hydrogen production are steam reforming, partial oxidation, oxidative steam reforming, and CO_2 reforming of different hydrocarbons [4-7]. Currently, steam reforming of natural gas is the most economical method for syngas production due to its abundance [8]. However, where infrastructure for natural gas processing has not been developed, liquefied petroleum gas (LPG) and propane as the main component of the LPG appear as more preferred feedstock for hydrogen production [9].

LPG is a by-product of gas processing and commercially available. In addition, propane can be readily liquefied under low pressure at ambient temperature. So it is very convenient for safe storage and transportation [10]. Nowadays, the demand for using feedstock with high volumetric hydrogen density is more prominent for fuel cell applications and on-board hydrogen production [11]. Propane is cleaner and contains a higher amount of hydrogen as compared with heavier hydrocarbons, including naphtha and diesel [9]. There are various pathways for hydrogen production from propane [12-14]. Studies have been focused on propane steam reforming (PSR) further through reaction (**1**) because steam can also be a hydrogen source, and more concentration of hydrogen can be yielded [9].

*Corresponding author.
E-mail address: golshanmazloom84@gmail.com (G. Mazloom)

$$C_3H_8 + 3H_2O \rightarrow 3CO + 7H_2 \ \Delta H^{\circ}_{298K} = 499kJ/mol \ (1)$$

Catalysts are based on non-noble metals, especially Ni, over different supports; alumina, zirconia, and ceria have been studied widely in PSR due to the high activity and cost-effectiveness [15-18]. However, coke formation is still a big problem for developing Ni-based catalysts. Adding another metal as a promoter is a common strategy considered by different researchers to improve the activity and stability of Ni-based catalysts [19]. Employing cerium and potassium as promoters are highly regarded [19, 20]. It has been reported that reducibility and active phase dispersion are promoted by ceria addition [21, 22]. Also, ceria can improve resistance against coke deposition through its high oxygen capacity [23, 24]. Based on the literature, potassium addition can change the acid-base properties of the catalyst in favor of water gas shift reaction (WGSR) and coke gasification in steam reforming reactions [20].

Due to some disadvantages accompanied by fixed bed reactor such as high-pressure drop, pore diffusion limitation, low heat conductivity, non-uniform temperature distribution, lack of continuity in the regeneration and replacement of the catalysts, development of these reactors on an industrial scale is limited. Besides catalyst improvement, different reactor technologies have been widely studied to improve different reforming processes and counteract possible defects (coke formation and low H_2 yield). Different reactor types have been proposed; microchannel reactors, monolith reactors, foam reactors, fixed bed membrane reactors, fluidized bed membrane reactors, fluidized bed, and circulating fluidized bed reactors [25-29]. Some specifications of the fluidized bed reactor, including small pressure drop, more efficient temperature control and negligible mass transfer limitations, make it a good candidate for reforming reactions. Shi et al. [26] studied the effects of operating parameters on the methanol steam reforming in the fluidized bed reactor. Khajeh et al. [28] have modeled the fixed bed and fluidized bed methane tri-reformers based on the mass and energy balances. The superiority of the fluidized bed was proved by an enhancement in feed conversions and hydrogen yield. Jing et al. [29] have shown that fluidization favors inhibiting deposited carbon and thermal uniformity in the reactor as compared with the fixed bed. However, the literature review has shown that fluidized bed reactors have been extensively studied for reforming of different gas and liquid hydrocarbons. But to our knowledge there are no literature data about the application of fluidized bed in PSR. In this study, the catalytic performance of Ni-K/CeO_2-Al_2O_3 catalyst in PSR was compared in fluidized and fixed bed reactors. The effects of promoters, space velocity, temperature and steam content on propane conversion, H_2 yield and stability were studied. Steam content was chosen under stoichiometric value which was in favor of coke deposition.

2. Experimental

2.1. Catalyst preparation

CeO_2-Al_2O_3 support was prepared by the impregnation of commercial Al_2O_3 (Merck) in an aqueous solution of $Ce(NO_3)_3.6H_2O$ (Merck) with an appropriate concentration and 80 °C followed by drying at 100 °C for 12 h and calcination at 700 °C for four h in air.

Ni-K/CeO_2-Al_2O_3 catalyst was prepared by the co-impregnation method [30, 31]. The synthesized CeO_2-Al_2O_3 powder was added to the solution included $Ni(NO_3)_2.6H_2O$ (Merck) and KNO_3 (Merck). After impregnation at 80 °C, the rest of the process was performed as described above. The Ce, Ni and K nominal content were chosen as 6 wt.%, 10 wt.% and 2 wt.%, respectively.

To evaluate, the effects of K and Ce on the catalytic performance, Ni/CeO_2-Al_2O_3, Ni-K/Al_2O_3 and Ni/Al_2O_3 were also synthesized with the above-mentioned preparation method and nominal content. The catalysts were sieved to the mean diameter of 120 μm. The Pycnometer was used for the determination of the specific gravity of the particles (3.4 g/cm^3).

2.2. Catalyst characterization

The structural characterization of the fresh catalyst was obtained by X-ray diffractometer (PW1730 Philips) in the range of 2θ = 10°–80°. The BET surface area, pore volume and pore size distribution of the used and the fresh catalysts were measured by N_2 adsorption and desorption isotherm at 77 K by an automated gas adsorption analyzer (BELSORP-mini II, BEL, Japan). The morphology of the spent catalysts was characterized by scanning electron microscopy (TESCAN VEGA/XMU). Calculation of the amount of carbon deposited on the used catalysts was carried out by TG-DTA analysis using STA504 (Bahr, Germany).

2.3. Reaction system

The fluidized bed reactor was a quartz tube with 11 mm internal diameter and 500 mm length. This tube is equipped with a distributor which is made of dense quartz wool. The reactor was placed in a vertical furnace. A PID controller joint with a K-type thermocouple was used for temperature control. The schematic of the fluidized bed set-up is shown in Fig. 1.

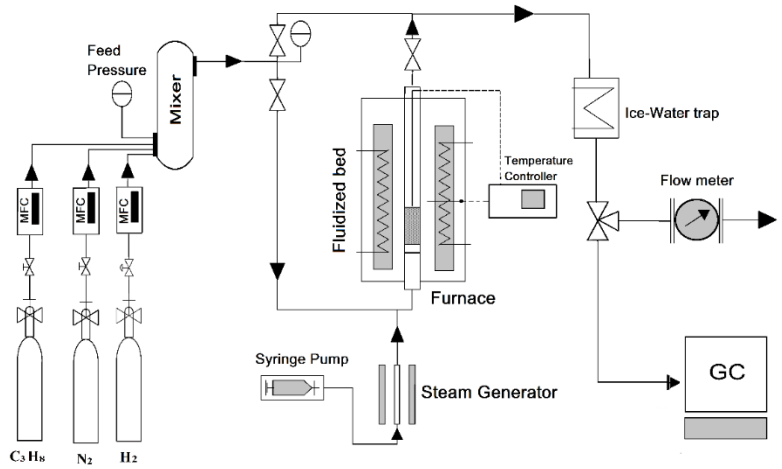

Fig. 1. Illustration of the fluidized bed set up schematically

The fixed bed reactor consisted of the same quartz tube installed in a horizontal furnace. The catalyst was placed between two layers of quartz wool in order to prevent catalyst movement.

In each run, 300 mg of catalyst was charged into the reactor and reduced with 35 mL/min H_2 flow at 750 °C and for 3 h. A mixture of C_3H_8 and N_2 with appropriate amounts was prepared as the reactor feed. A syringe pump was used to transfer water to the reactor. Water was converted to steam in preheater before entering into the reactor. The products and reactants composition were analyzed by on-line ThermoFinnigan (Model No. KAV00109) gas chromatograph (GC). The operating conditions of the experiments used in this study are shown in Table 1. The propane conversion, hydrogen yield, H_2/CO ratio and deactivation (Δx) were calculated as follows:

$$X_{C_3H_8} = \frac{F_{in.C_3H_8} - F_{out.C_3H_8}}{F_{in.C_3H_8}} \times 100 \qquad \textbf{(2)}$$

$$Y_{H_2} = \frac{F_{out.H_2}}{4 \times F_{in.C_3H_8} + F_{in.H_2O}} \times 100 \qquad \textbf{(3)}$$

$$\frac{H_2}{CO} = \frac{F_{out.H_2}}{F_{out.CO}} \qquad \textbf{(4)}$$

$$\Delta X = \frac{X_{C_3H_8.\max} - X_{C_3H_8.\min}}{X_{C_3H_8.\max}} \times 100 \qquad \textbf{(5)}$$

Where F_{in}, F_{out}, X and Y are inlet molar flow rate, outlet molar flow rate, conversion and yield of the component i, respectively.

Minimum fluidization velocity (U_{mf}) was estimated experimentally with N_2 at environment temperature. The bed pressure drop curve versus increasing and decreasing gas inlet velocity was measured. According to the Fig. 2, U_{mf} of 1.2 cm/s was determined where bed pressure drop did not change further with the gas velocity.

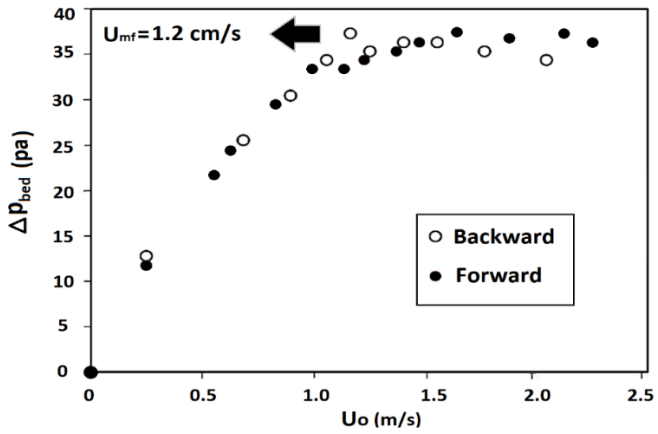

Fig. 2. Determination of $U_{mf.}$ For catalyst.

Table 1. The selected operating conditions

Variable	Range studied
Particle diameter, d_p	120 μm
Particle density, ρ_p	3.4 g/cm^3
Catalyst weight	300 mg
Temperature, T	600-750 °C
Relative velocity, U_0/U_{mf}	1-3
Gas hourly space velocity, (GHSV)	13600-41000 mL/(g.h)
Steam/propane, S/C	1.5, 2.5,3

3. Results and discussion

3.1. The characterization of the fresh catalyst

The XRD pattern of the fresh Ni-K/CeO_2-Al_2O_3 catalyst is shown in Fig. 3. The reflections of NiO (2θ= 37.3°,

43.3°, 62.9°, 75.5°), CeO_2 (2θ= 28.5°, 33.3°, 47.5°, 56.3°), K_2O (2θ= 63°) and Al_2O_3 (2θ= 67.3°) are clearly visible [32].

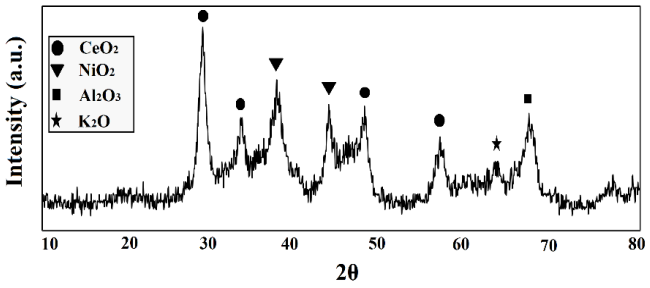

Fig. 3. The XRD pattern of the fresh Ni-K/CeO_2-Al_2O_3 catalyst

3.2. Catalytic performance

3.2.1. The effect of promoters

The activity and stability of all synthesized catalysts were investigated in fluidized- and fixed-bed reactors at T=650 °C, GHSV=27000 mL/ (h.g) and S/C= 3 for 7 h. The propane conversion and H_2 yield for the catalysts with different promoters as a function of reaction time are shown in Fig. 4. The amounts of deactivation (ΔX) obtained over different catalysts in fixed- and fluidized-bed reactors are presented in Table 2. All the fluidized bed catalysts exhibited more stable as well as more active performance compared to the fixed bed reactor. The results showed that both activity and stability were improved for the catalysts doped with Ce or K. However, the effects of promoters on stability were more pronounced. For example, for the fluidized bed reactor, a decrease in ΔX from 20.7% for Ni/Al_2O_3 to 10.1% and 7.6% was observed with the introduction of Ce and K, respectively. There are little differences between initial propane conversion obtained by K-doped and Ce-doped catalysts. While Ni-K/Al_2O_3 showed slightly higher H_2 yield than that of Ni/CeO_2-Al_2O_3.

The Ni-K/CeO_2-Al_2O_3 was more active than the others with higher propane conversion, higher H_2 yield and higher resistance for coke formation. It seems that the synergetic effects between metals resulted in the superior activity of Ni-K/CeO_2-Al_2O_3 catalyst.

Based on the literature review [20-24], ceria has high oxygen storage capacity, providing higher activity as well as higher resistance to coke formation. K doping promotes gasification and WGSR reactions and reduces the methanation reaction via effects on the acid-base properties of the catalyst. Also, Ni dispersion improves in the presence of K and Ce, due to the stronger metal-support interaction as well as preventing metal sintering.

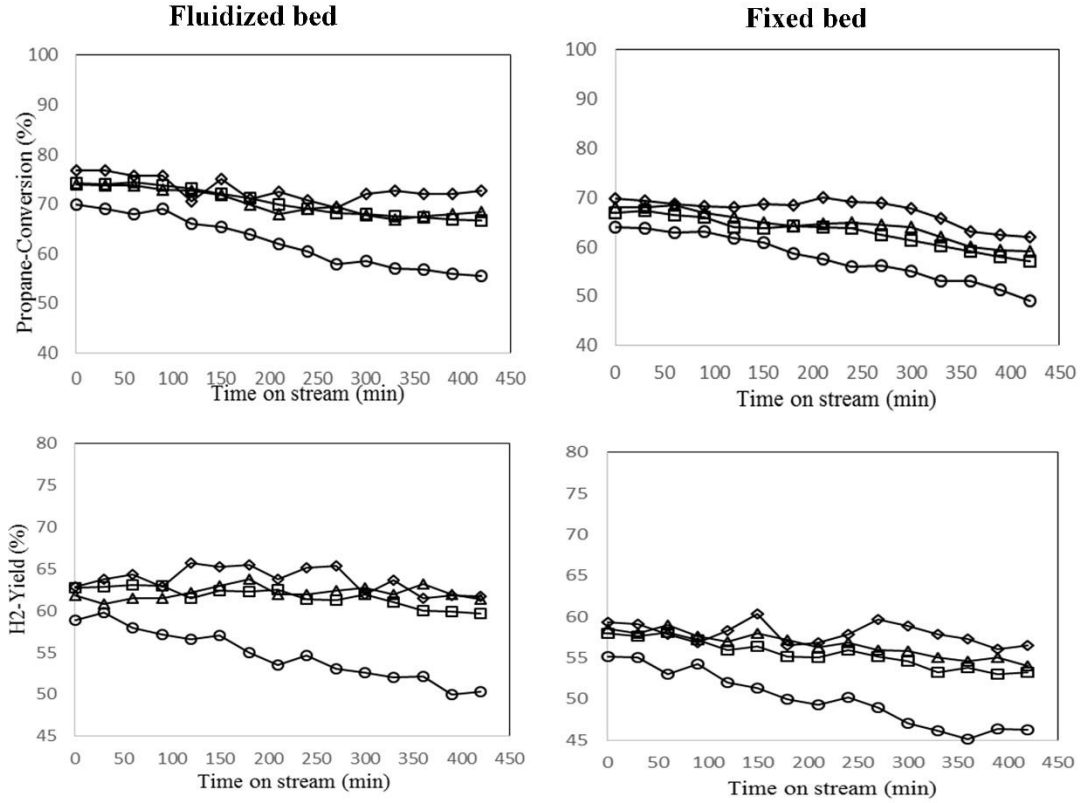

Fig. 4. Catalytic performance over ○)Ni/Al_2O_3, Δ)Ni-K/Al_2O_3, □) Ni/CeO_2-Al_2O_3, ◊)Ni-K/CeO_2-Al_2O_3. Reaction condition: T=650 °C, GHSV=27000 mL/(g.h) and S/C=3

Table 2. Amounts of different catalysts deactivation (%) at T=650 °C, GHSV=27000 mL/(g.h) and S/C=3

Catalyst	Fluidized bed	Fixed bed
Ni-K/CeO_2-Al_2O_3	2.6	7.8
Ni/Al_2O_3	20.7	23.4
Ni/CeO_2-Al_2O_3	10.1	14.6
Ni-K/Al_2O_3	7.6	13.2

3.2.2. The effect of feed flow rate

Fig. 5 indicates the effects of the space velocity on the propane conversion obtained over Ni-K/CeO_2-Al_2O_3 at both fluidized and fixed bed reactors. The GHSV was varied between 13600 to 41000 mL/(h.g) via changing the inlet gas flow rate (U_0/U_{mf}= 1-3) while the catalyst mass was kept constant. The other operating conditions were fixed at T=650 °C and S/C=2.5. At low space velocity, the obtained propane conversion was almost similar at both reactors indicating that particles did not fluidize well at low U_0. At higher space velocity, the propane conversion was obtained higher in the fluidized bed and the differences between two reactors became significant. Also decreasing the trend of propane conversion in the fluidized was not as much as in the fixed-bed. It may be due to the back-mixing phenomena in the fluidized bed which increase the residence time of gas in the catalytic bed [33]. In addition, increasing U_0 resulted in elevating gas-solid diffusion coefficient which increase gas-catalyst contact rate [34]. Based on Fig. 5, in other experiments in this work, the GHSV was fixed at 27000 mL/(h.g).

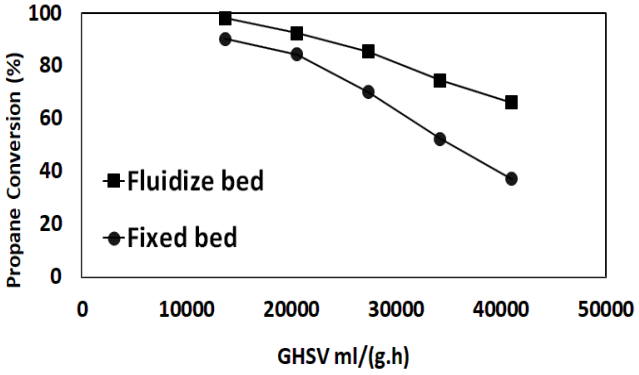

Fig. 5. Propane conversion obtained over Ni-K/CeO_2-Al_2O_3 at various GHSV. Reaction condition: T=650 °C, S/C=2.5

3.2.3. The effect of temperature

Fig. 6 indicates the effects of the temperatures on the propane conversion and H_2 yield obtained over Ni-K/CeO_2-Al_2O_3 at both fluidized and fixed bed reactors. The temperature was varied between 600 and 750 °C. This temperature range was selected based on the well-documented literature [35-37]. PSR is an endothermic reaction. Literature data have shown that hydrogen production is thermodynamically favored at the temperature zone of 800 to 1000 K for S/C ratio≤3 [38]. The other operating conditions were set at GHSV= 27000 mL/(g.h) and S/C=3. Fig. 6 shows that the propane conversion and H_2 yield decreased rapidly as the reaction temperature decreased due to the endothermic properties of PSR (eq. 1). Also, obtained propane conversion and H_2 yield were lower in the fixed bed reactor than those of the fluidized bed and a significant difference between two reactors in propane conversion and H_2 yield were observed at lower temperature.

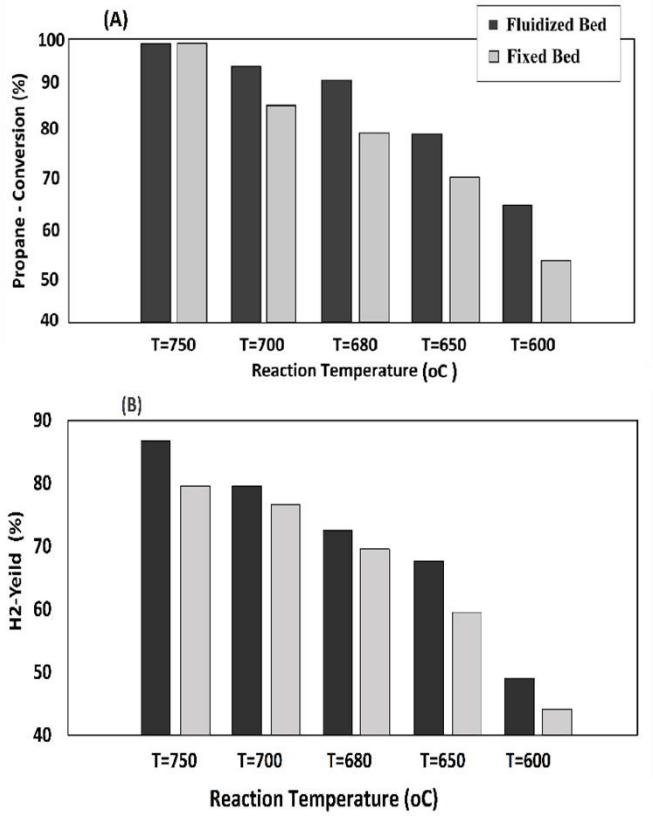

Fig. 6. A) Propane conversion and B) hydrogen yield obtained over Ni-K/CeO_2-Al_2O_3 at various temperatures. Reaction condition: GHSV= 27000 mL/(g.h) and S/C=3

Highly endothermic properties of PSR can lead to a non-uniform temperature distribution. This can cause negative effects on catalytic activity. Better performance of catalyst in the fluidized bed reactor can be assured due to the continuous circulating of the particles. Therefore, in the fluidized bed, higher heat and mass transfer rates can be achieved which limited the development of a significant temperature gradient.

A small amount of methane was also observed in the products. Fig. 7 presents the temperature dependencies

of the outlet mole fraction of CH_4 on dry basis. It can be seen that the methane concentration in two reactors was not much different. According to Fig. 7, the amount of methane outlet from the two reactors will be reduced significantly by increasing the reaction temperature. Because methane produced by propane –cracking reaction can participate in the reforming (eq. 6) and cracking (eq. 7) reactions at elevated temperatures.

At 750°C, the propane conversion in the two reactors was almost the same and approached the equilibrium, but the amount of hydrogen yield in the fluidized bed reactor was much higher. The difference in hydrogen yield at high temperatures may be related to the different reaction rate of the methane cracking (eq.7), methane steam reforming (eq.6) as well as the reaction of carbon oxidation (eq. 8) in the fixed- and fluidized-bed reactors.

Based on Fig. 6, in the stability tests in this work, the reaction temperatures were fixed at 600, 650 and 680 °C.

$$CH_4 + H_2O \leftrightarrow 3H_2 + CO \quad \Delta H^{\circ}_{298K} = 206 J/mol \qquad \textbf{(6)}$$

$$CH_4 \leftrightarrow 2H_2 + C \quad \Delta H^{\circ}_{298K} = 75 kJ/mol \qquad \textbf{(7)}$$

$$C + H_2O \leftrightarrow CO + H_2 \quad \Delta H^{\circ}_{298K} = 131 kJ/mol \qquad \textbf{(8)}$$

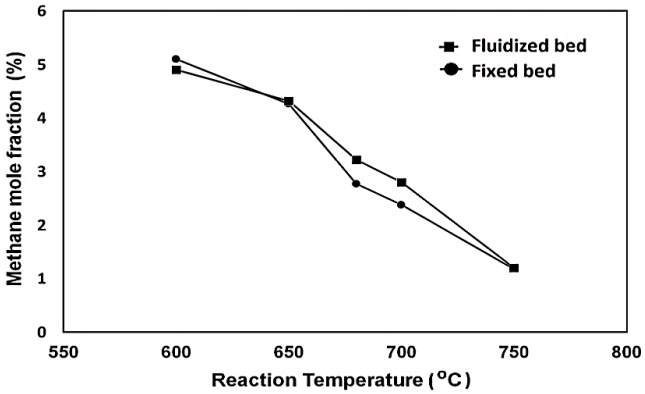

Fig. 7. Methane outlet mole fraction (on dry basis) obtained over Ni-K/CeO_2-Al_2O_3 at various temperature. Reaction condition: GHSV= 27000 mL/(g.h) and S/C=3

3.2.4. Stability test at different conditions

The stability of Ni-K/CeO_2-Al_2O_3 was examined by 7 h run time experiments in fluidized- and fixed bed reactors at similar operating conditions. The reaction conditions were: S/C=1.5, 2.5, 3, temperature= 600, 650, 680 °C and GHSV=27000 mL/(g.h). The propane conversion and H_2 yield as a function of reaction time are shown in Figs 8-10. The obtained H_2/CO ratio at different reaction conditions is shown in Table 3. The amounts of deactivation (based on eq. 5) at different conditions are presented in Table 4. Experiments at T=600 °C and S/C=1.5 were not carried out due to the low propane conversion.

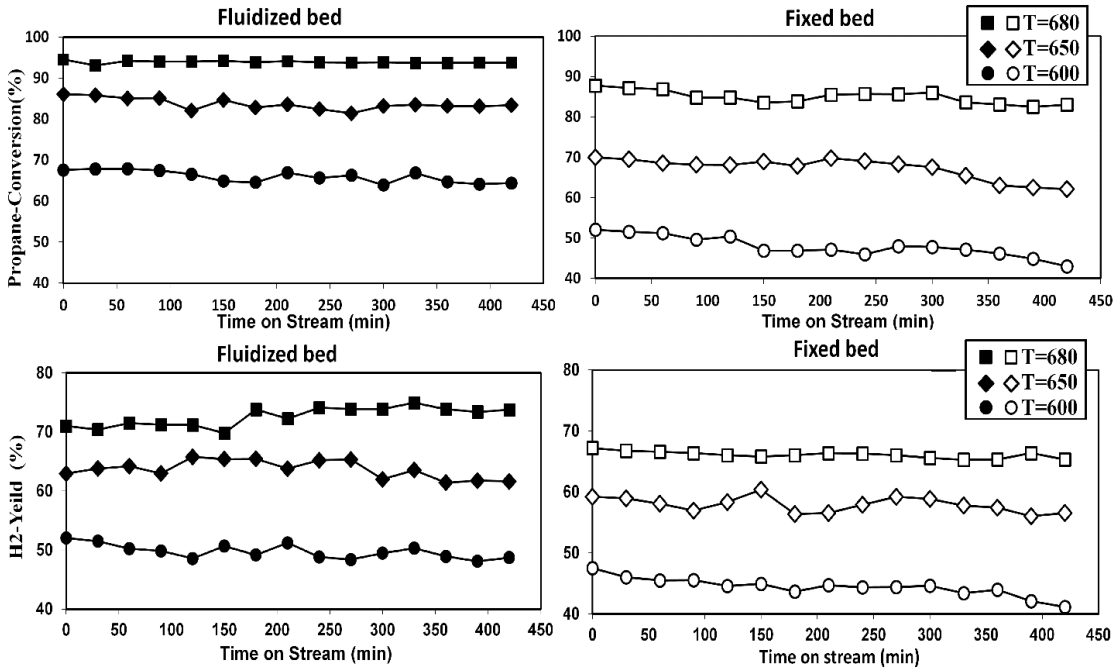

Fig. 8. The catalytic performance of Ni-K/CeO_2-Al_2O_3 at S/C=3. GHSV=27000 mL/(h.g)

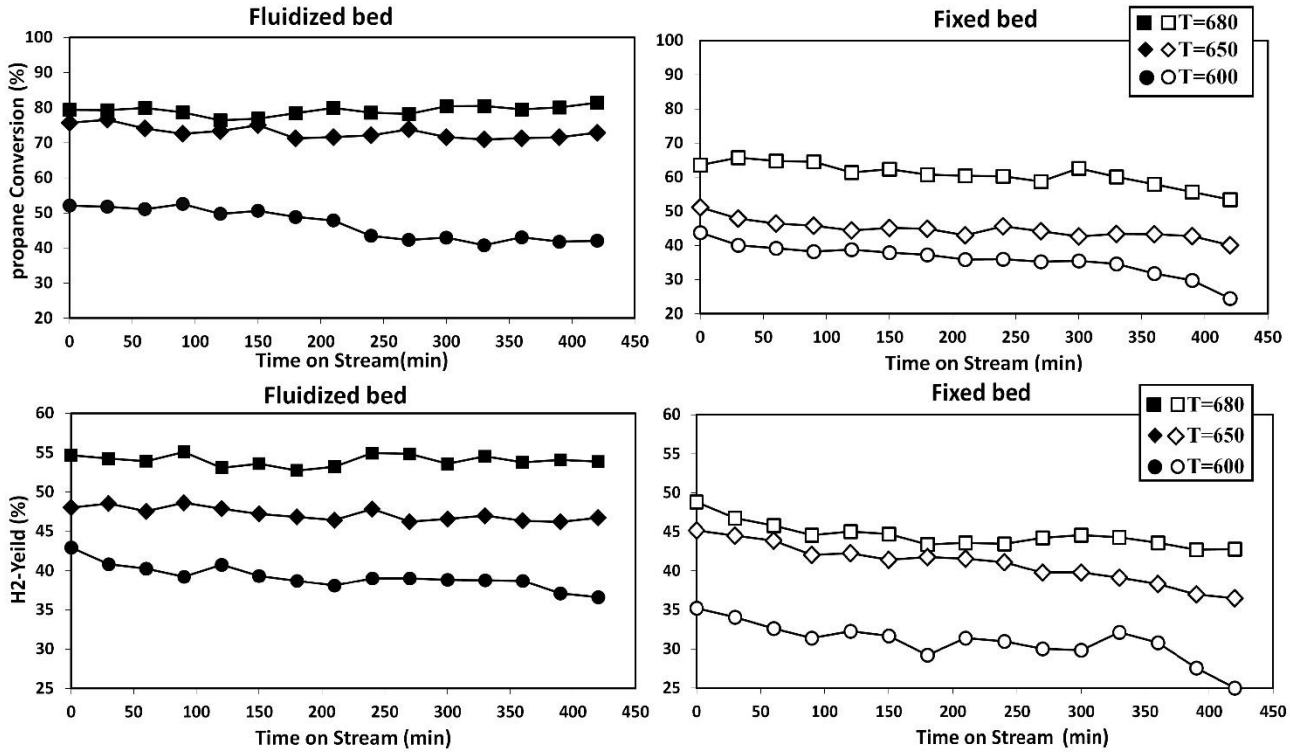

Fig. 9. The catalytic performance of Ni-K/CeO_2-Al_2O_3 at S/C=2.5. GHSV=27000 mL/(h.g)

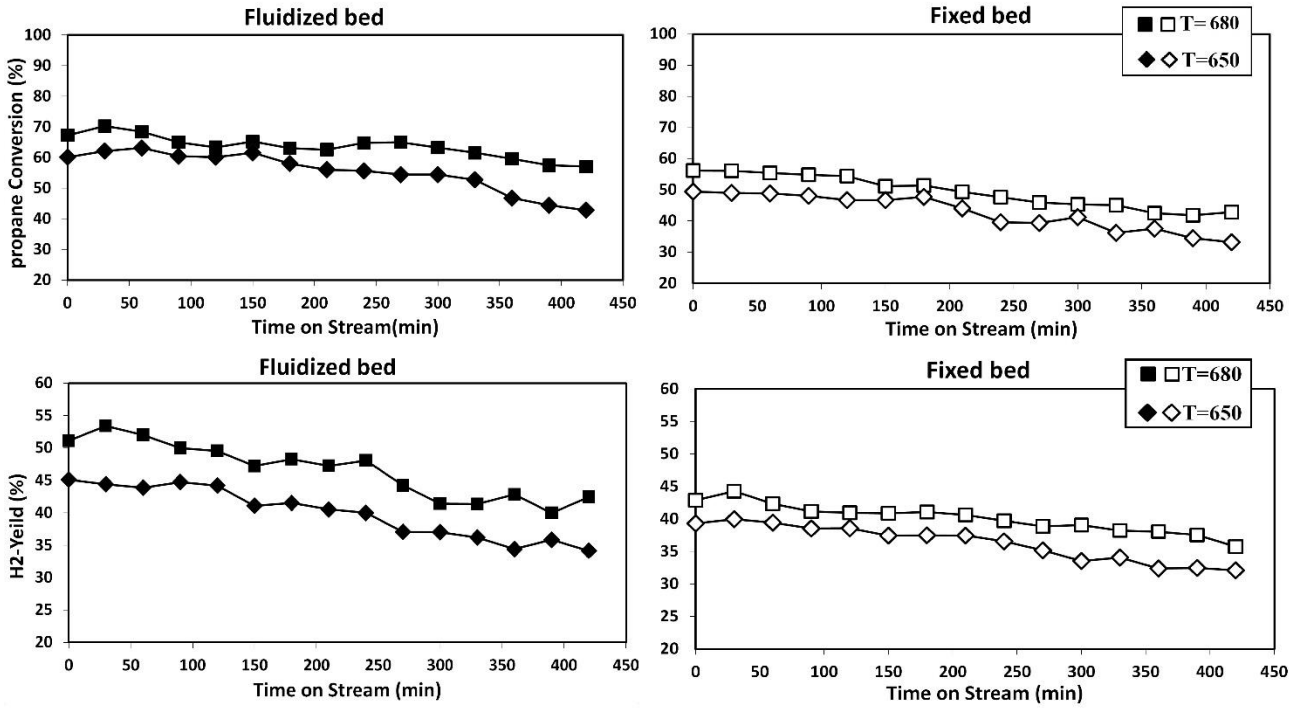

Fig. 10. The catalytic performance of Ni-K/CeO_2-Al_2O_3 at S/C=1.5. GHSV=27000 mL/(h.g)

Based on Figs. 8-10, increasing steam concentration improved H_2 yield as well as propane conversion. As shown in Table 3, with increasing temperature and decreasing steam content, H_2/CO ratio decreased in both the reactors. In the steam reforming reactions, the water gas shift reaction (WGSR, eq. 9) will also have a significant effect on the product distribution. The obtained results were in agreement with the fact that WGSR goes towards hydrogen production at lower temperature and higher steam content.

$$CO + H_2O \leftrightarrow CO_2 + H_2 \quad \Delta H^{\circ}_{298K} = -40kJ/mol \quad \textbf{(9)}$$

Table 3. Obtained H_2/CO ratio over Ni-K/CeO_2-Al_2O_3 at different reaction conditions. GHSV=27000 mL/(h.g)

Reactor	T (°C)	S/C=3		S/C=2.5		S/C=1.5	
		Initial H_2/CO	Final H_2/CO	Initial H_2/CO	Final H_2/CO	Initial H_2/CO	Final H_2/CO
Fluidized bed	680	2.1	2.4	1.8	1.7	1.5	1.3
Fluidized bed	650	2.6	2.7	2.4	3.0	2.3	2.7
Fluidized bed	600	3.5	3.9	5.0	4.2	4.5	4.0
Fixed bed	680	2.8	2.9	3.3	3.9	3.4	3.2
Fixed bed	650	3.7	3.8	5.0	4.0	4.5	4.1
Fixed bed	600	4.5	4.7	5.8	4.8	5.4	4.5

Figs. 8-10 show that the activity of the catalyst decreased steadily during 7 h on stream at both reactors. However, the higher stability was observed from the fluidized bed as compared to those from the fixed bed. TG/DTA and SEM analysis revealed coke deposition over all of the spent catalysts (section 3-3). Therefore, coke deposition has been considered as the main reason for the catalyst deactivation. Continuously circulated particles between oxidizing and reducing area in the fluidized bed lead to a lower coke formation and therefore lower deactivation (section 3-3). In addition, fluidization has positive effects on the more uniformly axial and radial temperature gradient and steam distribution.

Table 4. Amounts of Ni-K/CeO_2-Al_2O_3 deactivation at different conditions. GHSV=27000 mL/(h.g)

	T (°C)	$\Delta X(\%)$		
		S/C=3	S/C=2.5	S/C=1.5
Fluidized bed	680	0.8	1.0	9.2
Fluidized bed	650	2.6	4.7	20.8
Fluidized bed	600	3.4	10.0	---
Fixed bed	680	5.2	10.1	13.3
Fixed bed	650	7.8	12.1	18.2
Fixed bed	600	9.0	19.3	---

Also the decreasing trend of the catalytic activity postponed at both of the reactors with increasing temperature and steam content. The quantity of coke deposited on the samples was determined by the rate of gasification (eq. 8) and the rate of Boudouard reaction (eq. 10). It is expected that high temperature becomes an obstacle for Boudouard reaction. On the other hand, coke gasification is facilitated at a higher temperature and higher steam content. Therefore, in agreement with the obtained results in this work, higher temperature and higher steam content are not in favor of coke formation. Also Han et al. [33] reported that the rate of Boudouard reaction is relatively higher than the rate of coke gasification (eq. 8) in the fixed bed, while the opposite is true in the fluidized bed. This phenomenon was confirmed by the lower H_2/CO ratio observed in the fluidized bed compared to the fixed bed (Table 3).

$$2CO \leftrightarrow C + CO_2 \quad \Delta H^{\circ}_{298K} = -171 kJ/mol \quad \textbf{(10)}$$

Meanwhile the evaporation of water costs a great amount of heat. Therefore, too high S/C ratio should be avoided. In the fixed bed reactor, the deactivation of the catalyst occurred rapidly when steam content was lower than stoichiometric value. While the fluidization, especially when S/C=2.5 can compensate for the lack of water and enhance coke gasification which led to almost the stability of the catalyst. Fig. 10 shows that when steam content was too low (S/C=1.5) the catalyst at both reactors was deactivated and the distinction between the catalyst stability in both of the reactors was negligible. In the low steam content, fluidization did not occur in well quality due to the coke deposition and catalyst agglomeration (as can be seen in Fig. 11). Hence, it can be concluded that for PSR in this work, the ratio of S/C>1.5 is a critical condition for coke formation.

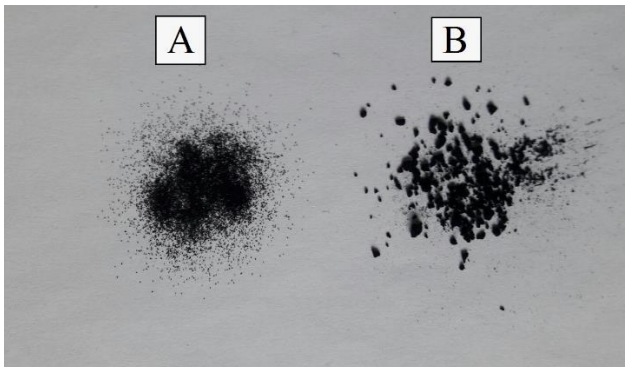

Fig. 11. Ni-K/CeO_2-Al_2O_3 Catalyst after 7 h being used in the fluidized bed A) S/C=3, B) S/C=1.5

3.2.5. Regenerability study of the catalyst

Coke accumulation over the catalyst is a big obstacle in the reforming reaction. Catalyst regeneration is carried out by coke gasification [39, 40]. Fan et al. [39] have examined the regenerability of Ni-Co/MgO-ZrO_2 catalyst under different environment air, N_2 and H_2 for 1 h. They reported that the deactivated catalyst can be regenerated by air.

In this work, after 7 h stability test in the fluidized bed reactor at T=600 °C, GHSV= 27000 mL/(h.g) and S/C=2.5, the used Ni-K/CeO_2-Al_2O_3 catalyst was regenerated in situ in the reactor under air atmosphere

for 1 h. The regenerated catalyst was tested again under the same reaction conditions as used in the stability test. As shown in Fig. 12, the deactivated catalyst was regenerated successfully. The initial catalytic activity was almost restored.

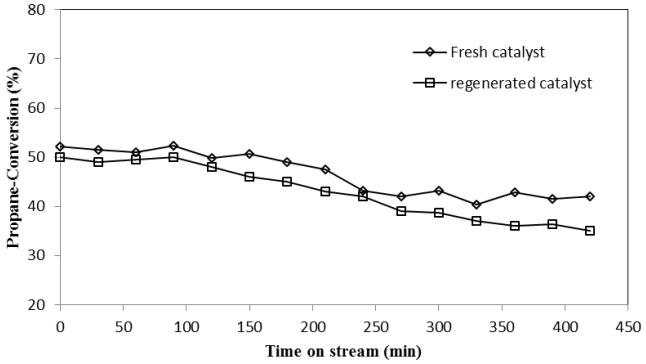

Fig. 12. Regenerability study of Ni-K/CeO_2-Al_2O_3 catalyst in the fluidized bed reactor. Reaction condition: T=600 °C, GHSV= 27000 mL/(h.g), S/C=2.5. Regeneration condition: air atmosphere, T=700 °C, GHSV= 27000 mL/(h.g)

3.3. The characterization of the spent catalysts

The morphology of the Ni-K/CeO_2-Al_2O_3 spent catalysts was characterized by SEM images, shown in Fig. 13. Coke filaments were clear over all of the samples. However, the amounts of the coke were strongly affected by the steam content and reactor type. It seems that the formation of filaments was more significant over the catalyst used in the fixed bed reactor. In addition, the filaments became longer and thicker with decreasing steam content.

The radial and axial distribution of steam is a very important factor affecting the structure and amount of coke. More uniform distribution of steam may be obtained in the fluidized bed due to the continuous circulation of solids. Therefore, oxidizing of coke was accelerated in the fluidized bed reactor. As a result, less and smaller coke was formed on fluidized bed catalysts [41].

Coke deposited over the Ni-K/CeO_2-Al_2O_3 catalyst after being used at different conditions was evaluated quantitatively by TG/DTA analysis. The results are presented in Figs. 14 and 15. The weight loss of the sample used in the fixed bed and S/C=3 was about 40% which increased to 60% by decreasing steam content to 1.5. In addition, the samples used in the fluidized bed revealed the lower weight loss than those of the fixed bed. By comparing two profiles of the fluidized bed samples, it seems that the S/C ratio was effective in the type rather than the amount of the coke deposited.

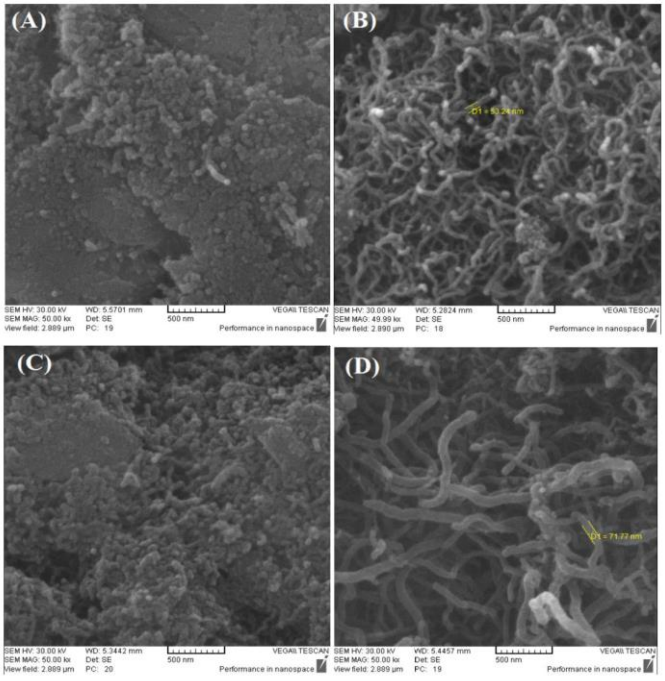

Fig. 13. SEM images of the spent Ni-K/CeO_2-Al_2O_3 catalyst. [T=650 °C, GHSV=27000 mL/(g.h)] A: Fluidized bed, S/C=3 B: Fixed bed, S/C=3 C: Fluidized bed, S/C=1.5 D: Fixed bed, S/C=1.5

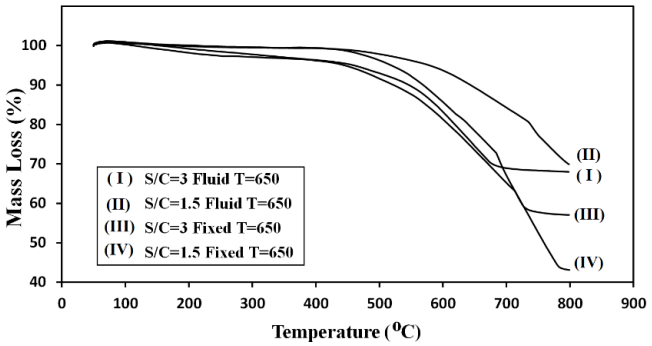

Fig. 14. TG results of the spent Ni-K/CeO_2-Al_2O_3 catalysts

The DTA profiles of all the samples are shown in Fig. 15. One shoulder at around 450 °C and a widespread peak at 500-800 °C were indicated in all the samples, attributed to the CH_x materials and coke filaments, respectively. There was little difference between the temperatures of the first peak which can be oxidized easier. With decreasing the S/C ratio as well as using the fixed bed reactor, the higher temperature peaks that can lead to catalyst deactivation [34] shifted to higher temperature. These observations were consistent with the obtained catalytic activity and stability (Figs. 8-10).

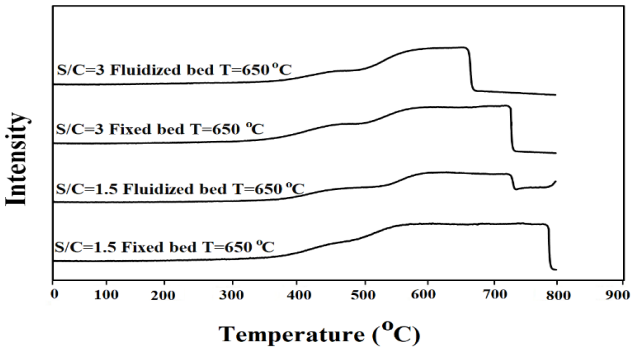

Fig. 15. DTA results of the spent Ni-K/CeO_2-Al_2O_3 catalysts

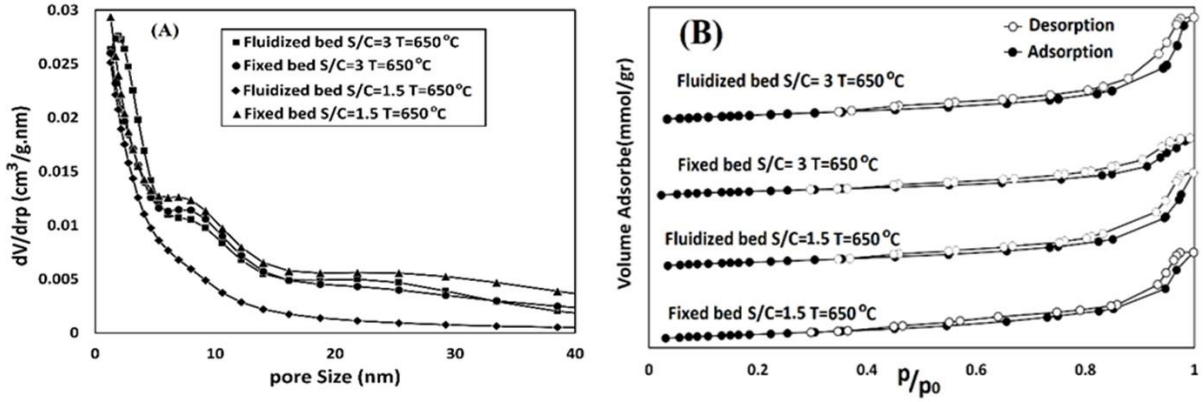

Fig. 16. A) N_2 adsorption-desorption isotherms B) Pore size distribution of the spent Ni-K/CeO_2-Al_2O_3 catalysts.

The textural properties of the used Ni-K/CeO_2-Al_2O_3 catalysts as well as the fresh one are shown in Table 5. Based on the results in Table 5, decreasing in surface area and pore volume accompanied by increasing pore diameter were observed over all of the spent catalysts as compared to the fresh one. It may be attributed to the coverage and blockage of the small pores by coke deposition. It seems that the conditions in which coke was produced further (based on the TGA analysis) were not in favor of surface area. Employing fixed bed reactor as well as lower S/C content led to decreasing surface area more intense in comparison with the fresh one.

High steam content and high reaction temperature can lead to the increasing the rate of active phase sintering [42]. Coke deposition and deactivation of the catalyst are accelerated due to the sintering. Because the interaction between the active phase and the support is weakened. The surface area can be related to the average equivalent particle size by the equation 11, where D_{BET} is the average diameter of a spherical particle in nm, S_{BET} represents the measured surface area of the powder in m^2/g, and ρ is the theoretical density in g/cm^3 [43]. The average equivalent particle sizes of different spent catalysts were calculated and compared in Table 5 with the fresh catalyst. The particle sizes of the spent catalysts in the fluidized bed were smaller than those of the spent catalysts in the fixed bed at the same temperature and steam concentration. Uniform distribution of temperature and steam in the fluidized bed reactor limited the sintering of the active phases.

$$D_{BET} = \frac{6000}{\rho S_{BET}} \quad \textbf{(11)}$$

Table 5. BET analysis of the Ni-K/CeO_2-Al_2O_3 catalyst before and after being used in the PSR

	T (°C)	S/C ratio	Surface area [a] (m^2/g)	Pore diameter [b] (nm)	Pore volume [b] (cm^3/g)	D_{BET} (nm)
Fluidized	650	3	98.0	8.5	0.29	18.0
Fixed	650	3	93.9	12.8	0.30	18.9
Fluidized	650	1.5	94.3	11.8	0.27	18.8
Fixed Fresh	650	1.5	92.1	13.5	0.28	19.1
	---	---	124.4	8.0	0.31	14.2

[a] Calculated by BET method, [b] Calculated by BJH method,

3.4. Comparison

Since the catalytic performance of fluidized bed in PSR has not been investigated. So far, the results obtained in this study were evaluated with the results of Ni based catalysts in similar systems in Table 6. As seen, Ni-K/CeO_2-Al_2O_3 catalyst in this work represented acceptable results.

Table 6. Comparison of the obtained results in this work with the Ni based catalysts in similar systems

Catalyst	Reactor	Temp. (°C)	Velocity	S/C	Conv.(%)	H_2 yield (%)	Coke deposition	Ref.
Ni-K/CeO_2-Al_2O_3	Fixed	650	27000 mL/(h.g)	3	70	60	40% weight loss after 7 h	This work
Ni-K/CeO_2-Al_2O_3	Fluidized	650	27000 mL/(h.g)	3	88	62	20% weight loss after 7 h	This work
NiO-$MgSiO_3$	Fixed	800	50000 mL/(h.g)	3	100	65	4.22 mg coke /g_{cat} after 20 h	[36]
10Ni-2La/SiO_2	Fixed	640	45000 mL/(h.g)	3	100	69	5% weight loss after 7 h	[44]
10Ni-3Ce/$MgAl_2O_4$	Fixed	600	30000 mL/(h.g)	3	94	62	10% weight loss after 7 h	[45]
10Ni/CeO_2 membrane: Pd/V/Pd	Membrane	500	124 mL/min	8.2	79.3	52.3	----	[46]

4. Conclusions

The catalytic performance of Ni-K/CeO_2-Al_2O_3 catalyst in propane steam reforming (PSR) was investigated in the fluidized- and fixed- bed reactors. The obtained propane conversion, H_2 yield, H_2/CO ratio and stability under different temperatures (650-680 °C) and steam concentration (steam/propane ratio (S/C) =3, 2.5 and 1.5) were compared and discussed. The operating conditions were selected to be suitable for coke formation. It was concluded that the fluidized bed was beneficial for PSR. Higher propane conversion, H_2 yield and a significant decrease in coke deposited were found in the fluidized bed. In the fixed bed reactor, the catalyst was deactivated rapidly when steam content was lower than the stoichiometric value. While it seems that the lack of water can be compensated by the circulation of the catalyst between different areas this improves coke gasification in the fluidized bed.

Acknowledgements

Authors gratefully acknowledge the financial support from (i) BRNS/DAE [37 (2)/14/20/2015], Govt. Of India (ii) DST-FIST/ Ministry of Science and Technology [SR/FST/CSI-273/2016], Govt of India and (iii) VGST KFIST Level-II, Dept. of IT, BT and S&T, Govt. of Karnataka, India.

References

[1] L.V. Mattos, G. Jacobs, B. H. Davis, F. B. Noronha, Chem. Rev. 112 (2012) 4094-4123.
[2] C. Agrafiotis, M. Roeb, C. Sattler, Renewable Sustainable Energy Rev. 42 (2015) 254-285.
[3] P. J. Woolcock, R. C. Brown, Biomass Bioenergy 52 (2013) 54-84.
[4] W. L. S. Faria, C. A. C. Perez, D. V. Cesar, L. C. Dieguez, M. Schmal, Appl. Catal. B 92 (2009) 217-224.
[5] C. F. Wu, L. Z. Wang, P. T. Williams, J. Shi, J. Huang, Appl. Catal. B 108–109 (2011) 6-13.
[6] W. H. Fang, S. Paul, M. Capron, F. Dumeignil, L. Jalowiecki-Duhamel, Appl. Catal. B 152–153 (2014) 370-382.
[7] S. F. Weng, Y. H. Wang, C. S. Lee, Appl. Catal. B. 134–135, (2013) 359–366.
[8] Y. Bang, J. G. Seo, I. K. Song, Int. J. Hydrogen Energy 36 (2011) 8307–8315.
[9] M. A. Rakib, J. R. Grace, C. J. Lim, S. E. H. Elnashaie, B. Ghiasi, Int. J. Hydrogen Energy 35 (2010) 6276-90.
[10] D. J. Haynes, D. Shekhawat, Dushyant S, Spivey JJ, David AB. Amsterdam: Elsevier (2011) 129-190.
[11] L. F. Brown, Int. J. Hydrogen Energy 26 (2001) 381-397.
[12] B. Johnston, M.C. Mayo, A. Khare, Technovation 25 (2005) 569-585.
[13] M. Ball, M. Wietschel, Int. J. Hydrogen Energy, 34 (2009) 615-627.
[14] M. B. Jensen, L. B. Raberg, A. O. Sjastad, U. Olsbye, Catal. Today, 145 (2009) 114-120.
[15] S. Ayabe, H. Omoto, T. Utaka, R. Kikuchi, K. Sasaki, Y. Teraoka, K. Eguchi, Appl. Catal. A 241 (2003) 261-269.
[16] H. R. Lee, K. Y. Lee, N. C. Park, J. S. Shin, D. J. Moon, B. G. Lee, Y. C. Kim, J. Nanosci. Nanotechnol. 6 (2006) 3396-3398.
[17] L. Zhang, X. Wang, B. Tan, U. S. Ozkan, J. Mol. Catal. A: Chem. 297 (2009) 26-34.
[18] S. Y. Park, J. H. Kim, D. J. Moon, N. C. Park, Y. C. Kim, J. Nanotechnol. 10 (2010) 3175-3179.

[19] M. Usman, W. W. Daud, H. F. Abbas, Renewable Sustainable Energy Rev. 45 (2015) 710-44.
[20] N. Yu, M. M. Rahman, J. Chen, J. Sun, M. Engelhard, P. Hernandez, Y. Wang, Catal. Today 323 (2019) 183-190.
[21] A. Trovarelli, Catal. Rev. 38 (1996) 439–520.
[22] S. B. Wang, G. Q. Lu, Appl. Catal. B. 19 (1998) 267–277.
[23] H. Wu, L. Wang, Catal. Commun. 12 (2011) 1374-1379.
[24] M. Tang, L. Xu, L. Fa, Int. J. Hydrogen Energy 39 (2014) 15482-15496.
[25] A. Delparish, A. K. Avci, Fuel Process. Technol. 151 (2016) 72-100.
[26] Y. Shi, X. Du, L. Yang, Y. Sun, Y. Yang, Int. J. Hydrogen Energy 38 (2013) 13974-13981.
[27] B. Arstad, J. Prostak, R. Blom, Chem. Eng. J. 189-190 (2012) 413-421.
[28] S. Khajeh, Z. Arab Aboosadi, B. Honarvar, J. Nat. Gas. Sci. Eng. 19 (2014) 152-160.
[29] Q. Jing, H. Lou, Li. Mo, X. Zheng, Energy Convers. Manag. 47 (2006) 459-469.
[30] A. Nandini, K.K. Pant, S. C. Dhingra, Appl. Catal. A 308 (2006) 119–127
[31] S. M. Masoom Nataj, S. M. Alavi, G. Mazloom, J. energy chem. 27 (2018) 1475-1488.
[32] W. Chen, G. Zhao, Q. Xue, Li. Chen, Y. Lu, Appl. Catal. B 136 (2013) 260-268.
[33] Y. K. Han, C. Ahn, J. W. Bae, A. Rong Kim, G.Y. Han, Ind. Eng. Chem. Res. 52 (2013) 13288-13296.
[34] C. E. Daza, A. Kiennemann, S. Moreno, R. Molina, Appl. Catal. A 364 (2009) 65-74.
[35] S. Barison, M. Fabrizio, C. Mortalò, P. Antonucci, V. Modafferi, R. Gerbasi, Solid state Ionics 181 (2010) 285–291
[36] F. Barzegari, M. Kazemeini, F. Farhadi, M. Rezaei, A. Keshavarz, Int. J. hydrogen energy 45 (2020) 6604-6620.
[37] K. M. Kim, B. S. Kwak, N. Park, T. J. Lee, S. T. Lee, M. Kang, J. Ind. Eng. Chem. 46 (2017) 324-336.
[38] X. Wang, N. Wang, J. Zhao, L. Wang, Int. J. hydrogen energy 35 (2010) 12800-12807
[39] M. S. Fan, A. Z. Abdullah, S. Bhatia, Appl. Catal. B 100 (2010) 365-377.
[40] Z. Shang, S. Li, L. Li, G. Liu, X. Liang, Appl. Catal. B 201 (2017) 302-309.
[41] Q. Jing, H. Lou, L. Mo, X. Zheng, Energy Convers. Manage. 47 (2006) 459-469.
[42] A. Carlos, S.C. Teixeira, R. Giudici, Chem. Eng. Sci. 54 (1999) 3609-3618.
[43] N. Hadian, M. Rezaei, Z. Mosayebi, F. Meshkani, J. Nat. Gas Chem. 21 (2012) 200-206.
[44] A.R. Aghamiri, S. M. Alavi, A. Bazyari, A. Azizzadeh Fard, Int. J. hydrogen energy 44 (2019) 9307-9315.
[45] A. Azizzadeh Fard, R. Arvaneh, S. M. Alavi, A. Bazyari, A. Valaei, Int. J. hydrogen energy 44 (2019) 21607-21622.
[46] M. Matsuka, K. Shigedomi, T. Ishihara, Int. J. hydrogen energy 39 (2014) 14792-14799.